The Journal of Immunology

De Novo–Induced Self-Antigen–Specific Foxp3 $^{+}$ Regulatory T Cells Impair the Accumulation of Inflammatory Dendritic Cells in Draining Lymph Nodes

Themis Alissafi, Aikaterini Hatzioannou, Marianna Ioannou, Tim Sparwasser, Joachim R. Grün, Andreas Grützkau and Panayotis Verginis

J Immunol 2015; 194:5812-5824; Prepublished online 6 May 2015;
doi: 10.4049/jimmunol.1500111
http://www.jimmunol.org/content/194/12/5812

The Journal of Immunology is published twice each month by
The American Association of Immunologists, Inc.,
1451 Rockville Pike, Suite 650, Rockville, MD 20852

Print ISSN: 0022-1767 Online ISSN: 1550-6606.

De Novo–Induced Self-Antigen–Specific Foxp3$^+$ Regulatory T Cells Impair the Accumulation of Inflammatory Dendritic Cells in Draining Lymph Nodes

Themis Alissafi,*,†,‡ Aikaterini Hatzioannou,‡ Marianna Ioannou,* Tim Sparwasser,§ Joachim R. Grün,¶ Andreas Grützkau,¶ and Panayotis Verginis‡

Foxp3$^+$ regulatory T cell (Treg)-based immunotherapy holds promise for autoimmune diseases. However, this effort has been hampered by major caveats, including the low frequency of autoantigen-specific Foxp3$^+$ Tregs and lack of understanding of their molecular and cellular targets, in an unmanipulated wild-type (WT) immune repertoire. In this study, we demonstrate that infusion of myelin in WT mice results in the de novo induction of myelin-specific Foxp3$^+$ Tregs in WT mice and amelioration of experimental autoimmune encephalomyelitis. Myelin-specific Foxp3$^+$ Tregs exerted their effect both by diminishing Ag-bearing inflammatory dendritic cell (iDC) recruitment to lymph nodes and by impairing their function. Transcriptome analysis of ex vivo–isolated Treg-exposed iDCs showed significant enrichment of transcripts involved in functional properties of iDCs, including chemotaxis-related genes. To this end, CCR7 expression by iDCs was significantly downregulated in tolerant mice and this was tightly regulated by the presence of IL-10. Collectively, our data demonstrate a novel model for deciphering the Ag-specific Foxp3$^+$ Treg-mediated mechanisms of tolerance and delineate iDCs as a Foxp3$^+$ Treg cellular target in unmanipulated mice. ***The Journal of Immunology*****, 2015, 194: 5812–5824.**

Regulatory T cells (Tregs) play an indispensable role in the maintenance of the immune homeostasis and the re-establishment of tolerance based on equivocal data both in mice and humans (1, 2). To this end, Treg-deficient mice develop lethal multiorgan autoimmunity, whereas in humans impaired Treg development leads to life-threatening autoimmune diseases (3–5). Although major effort has been placed in exploiting Tregs for therapeutic intervention in autoimmune diseases, in transplant rejection and allergy, this has been hampered by numerous caveats and impediments. First, emerging data suggest that the efficacy of Treg-mediated suppression is critically depended on Ag specificity. Because Ag-specific Tregs are infrequent in an unmanipulated repertoire (6), it is essential to devise protocols able to enhance their frequency either in vitro and/or in vivo. Second, growing knowledge supports the existence of diverse Treg subtypes with immunosuppressive potential, including natural Foxp3$^+$ Tregs, adaptive Foxp3$^+$ Tregs, and Tr1 regulatory cells (7, 8). The relative contribution of these Treg subsets in the maintenance of homeostasis and tolerance as well as the stability of their phenotype and function in vivo are ill defined (9). Finally, the molecular and cellular targets of the Treg-mediated suppression in an intact immune system remain elusive.

Accumulating data during the last decade have described multiple and diverse molecules and mechanisms to be involved in Foxp3$^+$ Treg-mediated suppression. These include 1) direct cell-to-cell contact-dependent mechanisms; to this end, expression of CTLA-4, gallectin-1, LAG-3, neuropilin1, and granzyme B by Tregs have all been shown to affect the function and/or survival of APCs and effector T cells; 2) secretion of immunosuppressive soluble mediators by Tregs, such as IL-10, TGF-β, and IL-35, which have been implicated in Treg suppressive activity; and 3) deprivation of IL-2, which may directly suppress effector T cell proliferation and function (1, 2, 10, 11). Although this knowledge has put the field a step forward, major questions regarding the relative contributions of the aforementioned mechanisms in Treg-mediated suppression in vivo as well as the specific cellular targets of Tregs remain unanswered. Importantly, experimental observations on Treg-mediated suppression have severe limitations, as they have been generated mainly using Tregs from either skewed TCR transgenic repertoires or gene-disrupted animals or via Ab-mediated elimination. Whether these data can be extrapolated to wild-type (WT) animals with an unmanipulated immune cell repertoire remains to be seen. Deciphering the relevant modes and targets of Treg-mediated suppression in a given inflammatory milieu in vivo in a WT immune cell repertoire would greatly advance the efforts toward the design of

*Institute of Molecular Biology and Biotechnology, Foundation for Research and Technology, 71300 Heraklion, Greece; †Laboratory of Autoimmunity and Inflammation, University of Crete Medical School, 71300 Heraklion, Greece; ‡Division of Clinical, Experimental Surgery, & Translational Research, Biomedical Research Foundation of the Academy of Athens, 11527 Athens, Greece; §Institute of Infection Immunology, TWINCORE, Centre for Experimental and Clinical Infection Research, 30625 Hannover, Germany; and ¶Deutsches Rheuma-Forschungszentrum, a Leibniz Institute, 10117 Berlin, Germany

Received for publication January 16, 2015. Accepted for publication April 5, 2015.

This work was supported by Greek General Secretariat of Research and Technology Grants Synergasia 09SYN-12-1074 and Aristeia II 3468 (to P.V.), European Union Project Innovative Medicine Initiative 6 ("BeTheCure") Contract 115142-2 (to P.V.). A.H. is supported by Greek General Secretariat of Research and Technology Grant Aristeia II 3468 (to P.V.), and T.A. is supported by the European Commission Seventh Framework Programme "Translational Potential" (TransPOT) under Contract 285948.

The chip data presented in this article have been submitted to the Gene Expression Omnibus under accession number GSE47210.

Address correspondence and reprint requests to Dr. Panayotis Verginis, Division of Clinical, Experimental Surgery, & Translational Research, Biomedical Research Foundation, Academy of Athens, 4 Soranou Efessiou Street, 11527 Athens, Greece. E-mail address: pverginis@bioacademy.gr

The online version of this article contains supplemental material.

Abbreviations used in this article: 7AAD, 7-aminoactinomycin D; DC, dendritic cell; DEREG, depletion of Treg; dLN, draining lymph node; dLNC, dLN cell; dpi, day postimmunization; DT, diphtheria toxin; EAE, experimental autoimmune encephalomyelitis; iDC, inflammatory DC; LN, lymph node; MOG, myelin oligodendrocyte glycoprotein; Treg, regulatory T cell; WT, wild-type.

www.jimmunol.org/cgi/doi/10.4049/jimmunol.1500111

customized Ag-specific Treg-mediated immunotherapies and ultimately the re-establishment of tolerance.

In this study, we demonstrate that infusion of a myelin Ag in unmanipulated WT mice results in de novo generation of myelin-specific Foxp3$^+$ Tregs and concomitant induction of self-tolerance. Furthermore, we identify Ag-bearing inflammatory DCs (iDCs) as the cellular target of the generated myelin-specific Foxp3$^+$ Tregs, because the latter reduce their accumulation in the draining lymph nodes (dLNs) of tolerant mice and impair their function. Finally, transcriptomic analysis of Treg-exposed iDCs revealed attenuated CCR7-mediated signaling that was dependent on the presence of IL-10. Overall, our data describe a novel model for induction of self-antigen–specific Foxp3$^+$ Tregs in WT animals and shed light on the mechanism of Ag-specific Treg-mediated suppression of autoimmune responses in an unmanipulated immune repertoire.

Materials and Methods

Mice

C57BL/6, BALB/c, and *Il10*$^{-/-}$ mice (C57BL/6 background), purchased from The Jackson Laboratory, depletion of Treg (DEREG) mice (C57BL/6 background), provided by Dr. Tim Sparwasser (Institute of Infection Immunology, TWINCORE, Hannover, Germany), *Foxp3gfp*.KI mice (C57BL/6 background), provided by Dr. Alexander Rudensky (Department of Immunology, Memorial Sloan-Kettering Cancer Center, New York, NY), and 2D2 TCR transgenic mice, provided by Dr. Lesley Probert (Hellenic Pasteur Institute, Athens, Greece), were used in this study. All procedures were in accordance with institutional guidelines and were approved by the Greek Federal Veterinary Office. All mice used in the experiments were 8- to 10-wk-old females.

In vivo protocols and experimental autoimmune encephalomyelitis induction

For peptide delivery, mice were implanted s.c. with osmotic micropumps (Alzet 1002; Durect) infusing 10 μg per day of myelin oligodendrocyte glycoprotein $(MOG)_{35–55}$ peptide (Genemed Synthesis) for 14 d. Mice were subsequently immunized s.c. at the base of the tail with 100 μg $MOG_{35–55}$ (Genemed Synthesis) or OVA (endograde V, Sigma-Aldrich) emulsified (1:1) in CFA (Sigma-Aldrich). Analysis was performed 12 d after immunization.

For experimental autoimmune encephalomyelitis (EAE) induction, mice were immunized s.c. at the base of the tail with 100 μg $MOG_{35–55}$ in CFA. Mice also received i.p. injections of 200 ng pertussis toxin (Sigma-Aldrich) at the time of immunization and 48 h later. Mice were monitored daily for clinical signs of disease as described (12). For depletion of Tregs, DEREG mice received i.p. 1 μg diphtheria toxin (DT; Sigma-Aldrich) 5 d before immunization.

For blocking of IL-10 signaling, mice received i.p. 250 μg IL-10R mAb (YL03 1B1.3a; rat IgG1κ [CA5], provided by Merck) 1 d prior and 1 d after $MOG_{35–55}$/CFA immunization and 125 μg on days 3 and 5 following immunization.

Flow cytometry and cell sorting

Single-cell suspensions were prepared from tissues and live cells (7-aminoactinomycin D [7AAD], BD Biosciences) were stained with conjugated Abs to CD11c (N418), CD11b (M1/70), Gr-1 (RB6-8C5), I-A^b (AF6-120.1), CD3e (145-2C11), CD19 (1D3), CD4 (RM4-5), CD8a (53-6.7), Vα3.2 (RR 3-16), Vβ11 (KT11), CD44 (IM7), CTLA-4 (CD152, UC10-4B9), LFA-1 (CD11a, M17/4), LAG-3 (CD223, C9B7W), GITR (CD357, DTA-1), CD25 (3C7), Helios (22F6), PD-L1 (10F.962), PD-L2 (DY25), CD80 (16-10A1), CD86 (GL-1), CD40 (3/23) (BioLegend), and CCR7 (CD197, EBI-1) (eBioscience). Foxp3 staining was performed using the Foxp3 (FJK-16s) staining set (eBioscience). For tetramer staining, 2×10^6 cells were incubated for 5 min with 10% mouse and rat sera (Jackson ImmunoResearch Laboratories) followed by 45 min staining with 10 μg/ml I-A^b/$MOG_{38–49}$ tetramer or I-A^b/hCLIP control tetramer (obtained from the National Institutes of Health Tetramer Facility) at room temperature. mAbs and viability dyes were added thereafter for 20 min on ice. For isolation of iDCs, dLNs and spleens were digested with collagenase D (2 mg/ml; Roche) for 30 min at 37°C. For the purification of total DCs, single-cell suspensions were incubated with Pan DC MicroBeads (Miltenyi Biotec) and then positively selected on a magnetic field according to the manufacturer's instructions (Miltenyi Biotec). For the purification of iDCs, positively selected DCs were stained with mAbs against CD11c, CD11b, and Gr-1. CD11c$^+$CD11b$^+$ Gr-1$^+$ cells were sorted on a high-speed MoFlo (Dako). Cell purity was ~85–95%.

For intracellular IL-10 staining, cells were isolated as described and stimulated in culture medium containing PMA (50 ng/ml, Sigma-Aldrich) and ionomycin (2 μg/ml, Sigma-Aldrich) for 4 h at 37°C. Brefeldin A (10 μg/ml, eBioscience) was added for 2 h. Following staining of surface markers cells were fixed with paraformaldehyde and permeabilized with 10% saponin buffer (Sigma-Aldrich). Cells were then incubated with IL-10 mAb (JES5-16E3, BioLegend). Cells were acquired on a FACSCalibur (BD Biosciences) and analyzed using FlowJo software (Tree Star).

For analysis of Ag uptake by DC subsets, mice were s.c. immunized with 100 μg OVA–Alexa Fluor 488 (Molecular Probes) in CFA. Then, 3.5 d later dLN cells (dLNCs) were isolated and stained for various DC subsets.

Adoptive transfer experiments

7AAD$^-$CD4$^+$Vα3.2$^+$Vβ11$^+$ $MOG_{35–55}$-specific T cells were sorted (purity >95%) from spleens and LNs of 2D2 transgenic mice, labeled with CFSE (Molecular Probes/Invitrogen; 10 μM for 20 min at 37°C in labeling buffer–PBS/0.1% BSA) and transferred (2×10^6 cells) i.v. into $MOG_{35–55}$-infused or control mice. At the same time, mice were s.c. immunized with $MOG_{35–55}$/CFA. dLNs and spleen were collected and analyzed 6 d after immunization.

Histological analysis and immunofluorescence

To assess CNS inflammation, mice were perfused with 4% paraformaldehyde. The spinal cords were dissected and fixed, followed by 30% sucrose. Fixed tissues were then frozen with OCT. Five-micrometer sections of the spinal cord were stained with H&E and analyzed in a blinded fashion.

For immunofluorescence staining, tissue was permeabilized by immersing the frozen sections in acetone for 10 min at −20°C. Sections were rinsed in PBS and blocked with 0.5% Triton X-100 solution for 60 min. Sections were then incubated overnight with rabbit anti-GFP Ab (1:500, Minotech Technologies). The next day sections were incubated for 1 h with anti-rabbit CF 488A IgG (1:800, Biotium). DAPI (300 nM, Sigma-Aldrich) fluorescent dye was used for nuclear staining.

T cell proliferation assays and cytokine assessment

Inguinal dLNs were harvested 9 d after immunization and 4×10^5 cells were cultured in the presence or absence of $MOG_{35–55}$ or OVA (30 μg/ml) for 72 h. Cells were then pulsed with 1 μCi ^{3}[H]thymidine (TRK120; Amersham Biosciences) for 18 h, and incorporated radioactivity was measured using a Beckman beta counter. Results are expressed as stimulation index defined as cpm in the presence of Ag/cpm in the absence of Ag. Cytokines were assessed in culture supernatants, collected after 48 h of stimulation. In other experiments sorted iDCs were stimulated with or without LPS (1 μg/ml; Sigma-Aldrich). Cytokines were assessed in supernatants, collected 18–20 h later. Pulsed iDCs (2×10^4) were then cultured in the presence of dLNCs (4×10^5) as responders, isolated from mice, 9 d following $MOG_{35–55}$/CFA immunization in the presence of $MOG_{35–55}$ peptide (30 μg/ml). Cytokines were assessed in culture supernatants 48 h later. In other experiments, 4×10^4 iDCs (isolated as described above) were cultured in a 1:1 ratio with CFSE-labeled (1 μM) dLNCs isolated from BALB/c mice in a MLR. In some experiments dLNs were dissected and homogenized with PBS containing protease inhibitors mixture (Roche). Detection of IL-2, IFN-γ (BD OptEIA, BD Biosciences), and CXCL1 (KC), TNF-α, IL-10, and IL-17 (DuoSet, R&D Systems) was performed by ELISA following the manufacturers' recommendations. In other experiments, inguinal LNs were dissected and homogenized with PBS containing protease inhibitors mixture (Roche). Detection of CCL19 and CCL21 (DuoSet, R&D Systems) in supernatants of dLN homogenates was performed by ELISA.

In vitro suppression assay

For in vitro suppression assays, 5×10^4 highly purified CD4$^+$Foxp3$^+$ Tregs were sorted from dLNs of $MOG_{35–55}$-immunized or tolerized/$MOG_{35–55}$-immunized *Foxp3gfp*.KI mice (7 d postimmunization [dpi]) and mixed with CellTrace-labeled CD4$^+$CD25$^-$CD62L$^+$ T cells isolated from naive B6 mice in a 1:1 ratio in the presence of Dynabeads mouse T-activator CD3/CD28 for T cell expansion and activation. Cells were collected and analyzed 4 d later.

GeneChip hybridization and data analysis

Total RNA from iDCs isolated from spleen and dLNs of tolerized/$MOG_{35–55}$-immunized or $MOG_{35–55}$-immunized mice 9 d following immunization was prepared with a Qiagen RNeasy mini kit. All experiments were repeated three times with individually sorted cells purified to >96% homogeneity. Hybridization on Affymetrix MG430 2.0 GeneChip arrays was performed at the Ramin gene array facility, and high-performance chip data analyses with the BioRetis database as well as hierarchical clustering were performed in the Bioinformatics Department of the German Rheumatism Research Center (Berlin, Germany) and validated as described (13). All chip data were uploaded to Gene Expression Omnibus (http://www.ncbi.nlm.nih.gov/geo, accession no. GSE47210) and are publicly available.

Quantitative PCR analysis

iDCs were isolated as described above, followed by reverse transcription with a ThermoScript reverse transcriptase kit (Invitrogen). Transcripts were quantified by incorporation of Platinum SYBR Green (Bio-Rad Laboratories) with a StepOnePlus real-time PCR system (Applied Biosystems), and expression was calculated by the change-in-threshold method ($\Delta\Delta C_T$) with *Hprt* mRNA (encoding hypoxanthine phosphoribosyltransferase 1). Specific primers were as follows: *Hprt*, forward, 5′-GTGAAACTGGAAAAGCCAAA-3′, reverse, 5′-GGACGCAGCAACTGACAT-3′; *Ccr7*, forward, 5′-GCTCCAGGCACGCAACTTT-3′, reverse, 5′-GACTACCACCACGGCAATGA-3′.

Western blot analysis

Whole-cell lysates (40 μg protein) were subjected to SDS-PAGE electrophoresis on 12% gels and then transferred to an Immobilon-P^{sq} membrane (Millipore). Membranes were blocked with 5% skimmed milk, 1% BSA, or 5% BSA in TBST and then incubated with anti–phospho-PI3K p85 (Tyr^{458})/p55 (Tyr^{199}) (1:1000, Cell Signaling Technology), anti-PI3K p85α (Z-8) (1:200, Santa Cruz Biotechnology), anti–phospho-Akt (Ser^{473}) (1:1000, Cell Signaling Technology), anti-Akt (C67E7) (1:1000, Cell Signaling Technology), anti–phospho-SAPK/JNK (Thr^{183}/Tyr^{185}) (1:1000, Cell Signaling Technology), anti-SAPK/JNK (1:1000, Cell Signaling Technology), anti–phospho-p38 MAPK (Thr^{180}/Tyr^{182}) (3D7) (1:1000, Cell Signaling Technology), and anti-p38 MAPK (1:1000, Cell Signaling Technology). Detection was performed using HRP-linked Abs (Cell Signaling Technology) and ECL detection reagents (Amersham Biosciences).

Statistical analysis

Statistical analyses were performed using a Student *t* test. Data are presented as means ± SEM. Differences were considered statistically significant at $p < 0.05$. All data were analyzed using GraphPad Prism v5 software.

Results

Subimmunogenic delivery of $MOG_{35–55}$ peptide in WT animals ameliorates EAE

The efficacy of Tregs in exerting their function is critically dependent on their Ag specificity (14, 15); however, Ag-specific Tregs are rare in an intact T cell repertoire. Others and we have previously demonstrated that subimmunogenic delivery of a foreign TCR agonist in WT animals leads to Ag-specific tolerance (16–18). To examine whether this method is suited for induction of self-tolerance, mice were infused with the self-peptide $MOG_{35–55}$ and monitored for EAE development. Notably, $MOG_{35–55}$-infused/$MOG_{35–55}$-immunized mice experienced significantly decreased severity and disease onset (Fig. 1A) and reduced inflammatory lesions in the spinal cords (Fig. 1B) as compared to $MOG_{35–55}$-immunized group. Specifically, assessment of spinal cord cell infiltrates using flow cytometry demonstrated a reduction of the frequency of $CD4^+$ and $CD8^+$ T cells as well as $CD11c^+$ DCs in $MOG_{35–55}$-infused/$MOG_{35–55}$-immunized compared to $MOG_{35–55}$-immunized mice. In contrast, the frequency of infiltrating $CD11c^-$ $Gr\text{-}1^+CD11b^{high}$ myeloid-derived suppressor cells (12, 19) was markedly enhanced (data not shown). In vitro recall stimulation assays of dLNCs isolated from $MOG_{35–55}$-infused/$MOG_{35–55}$-immunized mice showed a defective induction of IL-2, IFN-γ, and IL-17, accompanied by markedly reduced cell proliferation compared with control-immunized dLNCs (Fig. 1C). To address whether $MOG_{35–55}$ infusion tolerated specifically the self-reactive T cells, $MOG_{35–55}$-infused mice were immunized with OVA in CFA and dLNCs were restimulated in vitro with $MOG_{35–55}$ or OVA. Based on the production of IFN-γ and IL-17, the immunogenicity of OVA was not affected (Fig. 1D), suggesting that self-antigen infusion induces tolerance in an Ag-specific manner. Additionally, adoptive transfer of CFSE-labeled $MOG_{35–55}$-specific T cells ($V\alpha3.2^+V\beta8.1^+CD4^+$ cells), from 2D2 TCR transgenic mice, into $MOG_{35–55}$-infused/$MOG_{35–55}$-immunized mice demonstrated limited expansion and suppressed proliferation of the transferred cells in dLNs (Fig. 1E) and spleens (data not shown) compared with cells transferred into $MOG_{35–55}$-immunized animals. Overall, these results suggest that $MOG_{35–55}$ infusion induces self-tolerance and thus $MOG_{35–55}$-infused/$MOG_{35–55}$-immunized mice will be referred to henceforth as tolerized/$MOG_{35–55}$-immunized.

Infusion of $MOG_{35–55}$ peptide results in induction of $MOG_{35–55}$-specific $Foxp3^+$ Tregs

Next, we assessed whether infusion of $MOG_{35–55}$ peptide was accompanied by induction of $Foxp3^+$ Tregs. As shown in Fig. 2A, tolerized/$MOG_{35–55}$-immunized mice had significantly increased frequency and absolute numbers of $Foxp3^+$ Tregs in the dLNs as compared with $MOG_{35–55}$-immunized animals. Furthermore, application of the tolerization protocol to *Foxp3gfp*.KI mice revealed an enhanced frequency of $Foxp3^+$ Tregs within the inflammatory loci of spinal cords during the peak of EAE (Fig. 2B), suggesting that $Foxp3^+$ Tregs were enhanced in tolerized/$MOG_{35–55}$-immunized mice both in the peripheral lymphoid compartments as well as the target organ. Interestingly, assessment of $Foxp3^+$ Treg-associated molecules revealed significantly increased expression of CTLA-4 and LFA-1 on $CD4^+Foxp3^+$ cells of tolerized/$MOG_{35–55}$-immunized mice compared with control immunized animals, whereas expression of Helios, LAG-3, and GITR did not show noticeable differences between the two groups (Supplemental Fig. 1). Moreover, both $CD4^+Foxp3^+$ and $CD4^+Foxp3^-$ cell subsets exhibited elevated levels of IL-10, as was demonstrated upon intracellular staining of dLNCs from tolerized/$MOG_{35–55}$-immunized and control *Foxp3gfp*.KI immunized mice (Fig. 2C).

To determine whether infusion of $MOG_{35–55}$ results in induction of $MOG_{35–55}$-specific $Foxp3^+$ Tregs, we performed ex vivo staining of dLNCs using an $I\text{-}A^b$–restricted $MOG_{38–49}$-specific tetramer ($I\text{-}A^b/MOG_{38–49}$). Flow cytometry analysis revealed a significant increase in the proportion and absolute numbers of $I\text{-}A^b/MOG_{38–49}{}^+CD4^+Foxp3^+$ ($7AAD^-B220^-CD8^-$) cells in tolerized/$MOG_{35–55}$-immunized as compared with control-immunized mice and a marked contraction of the $I\text{-}A^b/MOG_{38–49}{}^+CD4^+Foxp3^-$ population (Fig. 2D). Finally, we assessed the in vitro suppressive potential of $Foxp3^+$ Tregs and $Foxp3^-CD4^+$ T cells isolated from tolerized/$MOG_{35–55}$-immunized and control-immunized *Foxp3gfp*.KI mice. Notably, $Foxp3^+$ Tregs from tolerized or control animals potently suppressed the proliferation of effector cells (Fig. 2E), whereas $Foxp3^-CD4^+$ T cells from the respective groups were unable to inhibit T cell proliferation (Supplemental Fig. 2). Overall, our data provide evidence for the induction of $MOG_{35–55}$-specific $Foxp3^+$ Tregs through infusion of $MOG_{35–55}$ autoantigen in WT mice that are potently suppressive.

Depletion of $MOG_{35–55}$-specific $Foxp3^+$ Tregs restores autoimmune reactivity in tolerant mice

The increased frequency of $MOG_{35–55}$-specific $Foxp3^+$ Tregs in tolerized/$MOG_{35–55}$-immunized mice indicates a potential role of

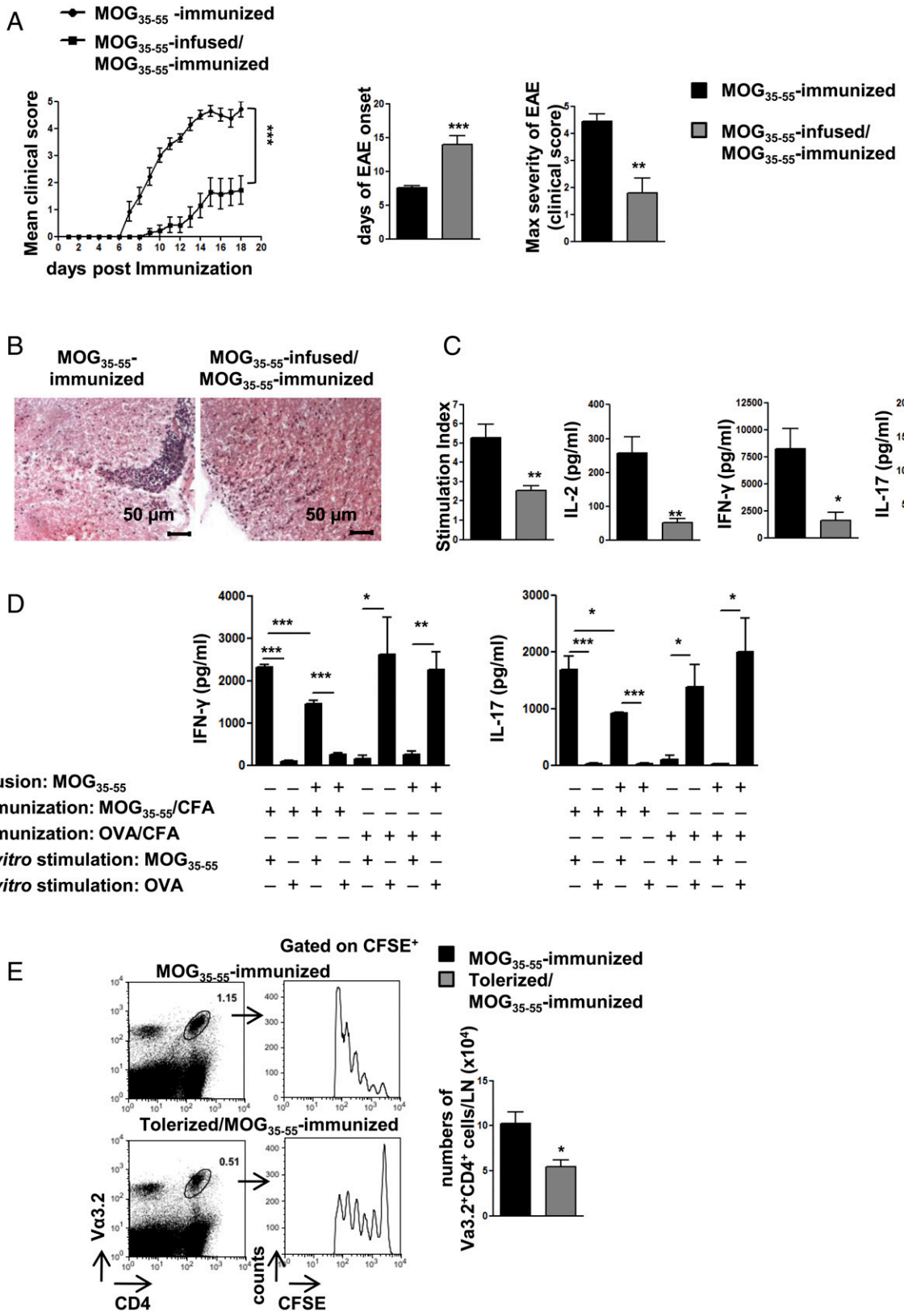

FIGURE 1. Induction of self-tolerance in $MOG_{35–55}$-infused WT animals. (**A**) Mean clinical score (***$p < 0.0001$), days of onset (***$p = 0.0004$), and EAE severity (**$p = 0.0011$) are shown. (**B**) Representative H&E sections from spinal cords of $MOG_{35–55}$-immunized (clinical score 4) and $MOG_{35–55}$-infused/$MOG_{35–55}$-immunized (clinical score 1.5) mice 14 dpi. (**C**) Stimulation index (**$p = 0.0055$) and IL-2 (**$p = 0.0021$), IFN-γ (*$p = 0.0109$), and IL-17 (**$p = 0.0035$) levels in supernatants of dLNCs (isolated 9 dpi) cultured with $MOG_{35–55}$. (**D**) dLNCs isolated from $MOG_{35–55}$-infused mice immunized with either $MOG_{35–55}$ or OVA were stimulated in vitro as shown. Levels of IFN-γ (***$p < 0.0001$, **$p = 0.0096$, *$p = 0.0206$) and IL-17 (***$p = 0.0006$, ***$p < 0.0001$, *$p = 0.0483$, *$p = 0.0126$, *$p = 0.0289$) are depicted. (**E**) Flow cytometric analysis of dLNCs (6 dpi) for CFSE dilution upon transfer of CFSE-labeled $Vα3.2^+Vβ8.1^+CD4^+$ 2D2 T cells in $MOG_{35–55}$-immunized or $MOG_{35–55}$-infused/$MOG_{35–55}$-immunized mice (gates were set on $CFSE^+$ cells). Numbers of $Va3.2^+CD4^+$ 2D2 cells per dLN (*$p = 0.0314$) are depicted. Results are expressed as means ± SEM; $n = 4$ mice/group, three independent experiments. For (A)–(C), results are expressed as means ± SEM; $n = 8$ mice/group, three independent experiments.

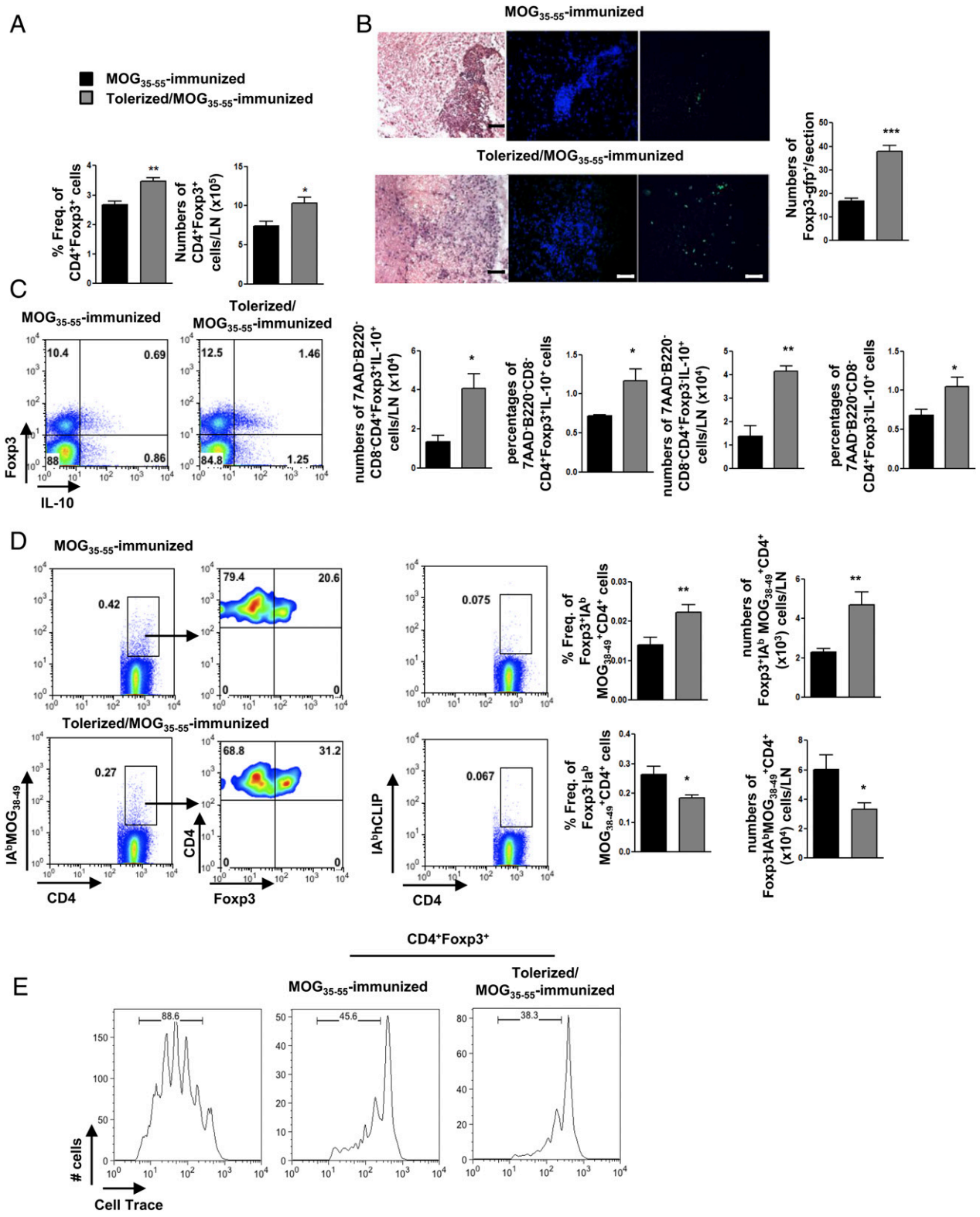

FIGURE 2. $MOG_{35–55}$ infusion leads to $MOG_{35–55}$-specific $Foxp3^+$ Treg induction. (**A**) Frequencies (**$p = 0.0014$) and numbers (*$p = 0.0111$) of $CD4^+$ $Foxp3^+$ dLNCs from $MOG_{35–55}$-immunized or tolerized/$MOG_{35–55}$-immunized mice, respectively (7 dpi). (**B**) Representative H&E and immunofluorescent sections from spinal cords of $MOG_{35–55}$-immunized (clinical score 4, 14 dpi) and tolerized/$MOG_{35–55}$-immunized (clinical score 2.5, 17 dpi) *Foxp3gfp*.KI mice. Scale bars, 50 μm. Numbers of Foxp3-GFP^+ cells per section are shown (***$p < 0.0001$). (**C**) Flow cytometric analysis of IL-10 expression by $CD4^+$ T cells isolated from dLNs of *Foxp3gfp*.KI mice. Numbers (*$p = 0.0131$) and percentages (*$p = 0.0163$) of $7AAD^-B220^-CD8^-CD4^+Foxp3^+IL\text{-}10^+$ cells per dLN are shown, as are numbers (**$p = 0.0050$) and percentages (*$p = 0.0423$) of $7AAD^-B220^-CD8^-CD4^+Foxp3^-IL\text{-}10^+$ cells per dLN. (**D**) Flow cytometric analysis of $CD4^+MOG_{38–49}$/$I\text{-}A^{b+}$ dLNCs from $MOG_{35–55}$-immunized or tolerized/$MOG_{35–55}$-immunized mice for the expression of Foxp3. hCLIP/$I\text{-}A^b$ was used as control. Frequencies (**$p = 0.0075$, *$p = 0.0299$) and numbers (**$p = 0.0039$, *$p = 0.0232$) of $CD4^+MOG_{38–49}$/$I\text{-}A^{b+}$ $Foxp3^+$ and $Foxp3^-$ cells, respectively, are shown. (**E**) $CD4^+Foxp3^+$ Tregs isolated from dLNs of $MOG_{35–55}$-immunized or tolerized/$MOG_{35–55}$-immunized *Foxp3gfp*.KI mice (7 dpi) were mixed with CellTrace-labeled $CD4^+CD25^-CD62L^+$ T cells (1:1 ratio) in the presence of CD3/CD28 Dynabeads. Flow cytometric analysis for CellTrace dilution was measured 4 d later. Results are expressed as means ± SEM; $n = 4$ mice/group, three (*Figure legend continues*)

these cells in the amelioration of EAE. To explore this hypothesis, we performed the tolerization protocol in DEREG mice (Fig. 3A) that express a DT receptor under the Foxp3 promoter. Injection of DT in tolerized animals eliminated the entire Foxp3-expressing Treg compartment (including Foxp3$^+$ Tregs induced during the infusion protocol) (data not shown). Mice were challenged with $MOG_{35–55}$/CFA 5 d later (Fig. 3A). At this time point only thymus-derived Tregs emerged in the periphery, because de novo generation of Foxp3$^+$ Tregs was not feasible (completion of $MOG_{35–55}$ infusion takes place in 14 d). Consistent with our previous findings, tolerized/$MOG_{35–55}$-immunized DEREG mice exhibited significantly decreased incidence of EAE that was markedly enhanced in tolerized/Foxp3$^+$ Treg-depleted/$MOG_{35–55}$-immunized mice (Fig. 3B). Additionally, robust secretion of IFN-γ and IL-17 as well as heightened T cell proliferation were observed in recall in vitro assays of dLNCs isolated from tolerized/Foxp3$^+$ Treg-depleted/$MOG_{35–55}$-immunized DEREG mice as compared with cells obtained from tolerized/$MOG_{35–55}$-immunized mice (Fig. 3C). Collectively, our data demonstrate the operation of dominant tolerance executed by myelin-specific Foxp3$^+$ Tregs in tolerized mice. Overall, our model provides a novel tool for delineation of mechanisms involved in Treg-mediated tolerance in an unmanipulated immune system.

Impaired migration and function of Ag-bearing inflammatory DCs in dLNs of tolerized/$MOG_{35–55}$-immunized animals

Extensive literature implicates DCs as one of the major cell targets of Treg-mediated suppression (2, 10, 11), but the precise DC subset that is targeted by Foxp3$^+$ Tregs remains elusive. Interestingly, we identified 7AAD$^-$CD3$^-$CD19$^-$CD11c$^+$CD11b^{high} Gr-1$^+$ DCs to be markedly decreased in the dLNs of tolerized/$MOG_{35–55}$-immunized animals as compared with $MOG_{35–55}$-immunized control mice (Fig. 4A). To determine whether the reduced CD11c$^+$CD11b^{high}Gr-1$^+$ DC accumulation to the dLNs was due to de novo–generated Foxp3$^+$ Tregs, we performed the Foxp3$^+$ Treg elimination protocol in tolerized/$MOG_{35–55}$-immunized DEREG mice as described in Fig. 3A. Notably, depletion of Foxp3$^+$ Tregs resulted in complete restoration of CD11c$^+$CD11b^{high}Gr-1$^+$ DC trafficking to the dLNs, because both their frequencies and absolute numbers reached the levels of the control-immunized littermates (Fig. 4B), suggesting that Foxp3$^+$ Tregs curtail the accumulation of CD11c$^+$CD11b^{high} Gr-1$^+$ DCs to the dLNs. Of note, the proportion of annexin V$^+$ CD11c$^+$CD11b^{high}Gr-1$^+$ DCs did not differ between tolerized/$MOG_{35–55}$-immunized and control-immunized mice (data not shown). Furthermore, kinetic experiments demonstrated an impaired accumulation of CD11c$^+$CD11b^{high}Gr-1$^+$ DCs in tolerized/$MOG_{35–55}$-immunized mice (Fig. 4C), suggesting that Treg-mediated cell death of CD11c$^+$CD11b^{high}Gr-1$^+$ DCs could not account for their impaired accumulation in dLNs of tolerized/$MOG_{35–55}$-immunized mice.

DCs expressing such phenotype have been characterized as iDCs (20–22) with a potent ability to augment T cell responses. Characterization of the function of iDCs in our setting demonstrated that iDCs isolated from $MOG_{35–55}$-immunized dLNs secreted vast amounts of proinflammatory cytokines such as CXCL1 and TNF-α (Fig. 5A), and they significantly enhanced $MOG_{35–55}$-specific Th1 and Th17 responses in vitro (Fig. 5B), thus confirming their inflammatory properties. Importantly, immunization of mice with OVA–Alexa Fluor 488/CFA demonstrated that Ag was mostly displayed by iDCs in the dLNs, whereas other CD11c-expressing cells only slightly contributed in Ag transport to dLNs (Fig. 5C).

To examine whether Foxp3$^+$ Tregs regulated not only the accumulation but also the phenotype and function of the remaining iDCs in the dLNs, we first assessed the expression of MHC class II and costimulatory or inhibitory molecules. Expression of I-A^b and CD86 molecules was significantly downregulated in DCs isolated from dLNs of tolerized/$MOG_{35–55}$-immunized mice compared with either tolerized/Foxp3$^+$ Treg-depleted/$MOG_{35–55}$-immunized or control $MOG_{35–55}$-immunized animals (Fig. 5D), whereas expression of CD80, CD40, PD-L1, and PD-L2 was not affected (Fig. 5D). Furthermore, iDCs isolated from dLNs of tolerized/$MOG_{35–55}$-immunized mice (H-2^b) were not as sufficient as iDCs from $MOG_{35–55}$-immunized or Foxp3$^+$ Treg-depleted/$MOG_{35–55}$-immunized syngeneic mice to induce activation, proliferation, and IL-2 release in an MLR using dLNCs from BALB/c (H-2^d) mice (Fig. 5E). Overall, our findings suggest that de novo–induced Foxp3$^+$ Tregs affect the recruitment of iDCs in the dLNs and potently modulate their function.

$MOG_{35–55}$-specific Foxp3$^+$ Tregs impair the accumulation of iDCs in the dLNs via downregulation of CCR7 expression

To gain insight into the mechanisms underlying Treg-mediated modulation of iDC function, we determined the gene expression pattern of iDCs from tolerized and control-immunized mice using Affymetrix expression microarrays. Surprisingly, 5155 differentially regulated transcripts were identified in iDCs from tolerized mice (data not shown). Hierarchical clustering, using Genes@Work with Pearson correlation and center of mass, pointed to an enrichment of genes encoding molecules involved in chemotaxis (for example *Ccr7*) (Fig. 6A), suggesting that tolerance induction through $MOG_{35–55}$-specific Foxp3$^+$ Tregs can regulate pathways critical for iDC migration to dLNs. To validate the microarray results, we performed quantitative real-time PCR for *Ccr7*. *Ccr7* expression by iDCs isolated from tolerized/$MOG_{35–55}$-immunized animals was found significantly reduced (Fig. 6B). Trafficking of DCs in dLNs is tightly regulated through interactions of LN stroma–derived CCL19 and CCL21 chemokines and CCR7 expressed by DCs (22, 23). To this end, we assessed whether $MOG_{35–55}$ infusion affected the secretion of these two chemokines. No significant differences were observed for CCL19, whereas CCL21 levels were increased in tolerized/$MOG_{35–55}$-immunized dLN homogenates (Fig. 6C). Our data indicate that $MOG_{35–55}$-specific Foxp3$^+$ Tregs impair the accumulation of iDCs in the dLNs via downregulation of CCR7 expression.

Inhibition of IL-10 signaling in tolerized/$MOG_{35–55}$-immunized animals restores iDC trafficking to the dLNs

Immunomodulatory cytokines such as IL-10 have been linked to Treg suppressive function (24–26). To examine whether the elevated secretion of IL-10 by Tregs was involved in the decreased accumulation of iDCs to dLNs of tolerized mice, we administered an IL-10R neutralizing Ab following completion of $MOG_{35–55}$ infusion (Fig. 7A). Neutralization of IL-10R signaling resulted in a 3-fold induction in the proportion of iDCs in dLNs of tolerized/$MOG_{35–55}$-immunized/IL-10R–treated mice compared with the tolerized/$MOG_{35–55}$-immunized group (Fig. 7B). Interestingly, blocking of IL-10R signaling in tolerized/$MOG_{35–55}$-immunized mice resulted in the upregulation of the expression of *Ccr7* (Fig. 7C) compared with tolerized/$MOG_{35–55}$-immunized animals,

independent experiments. For (A) and (B), results are expressed as means ± SEM; n = 8 mice/group, three independent experiments. For (C) and (D), dLNs were analyzed 7d following immunization and results are expressed as means ± SEM; n = 6 mice/group, three independent experiments.

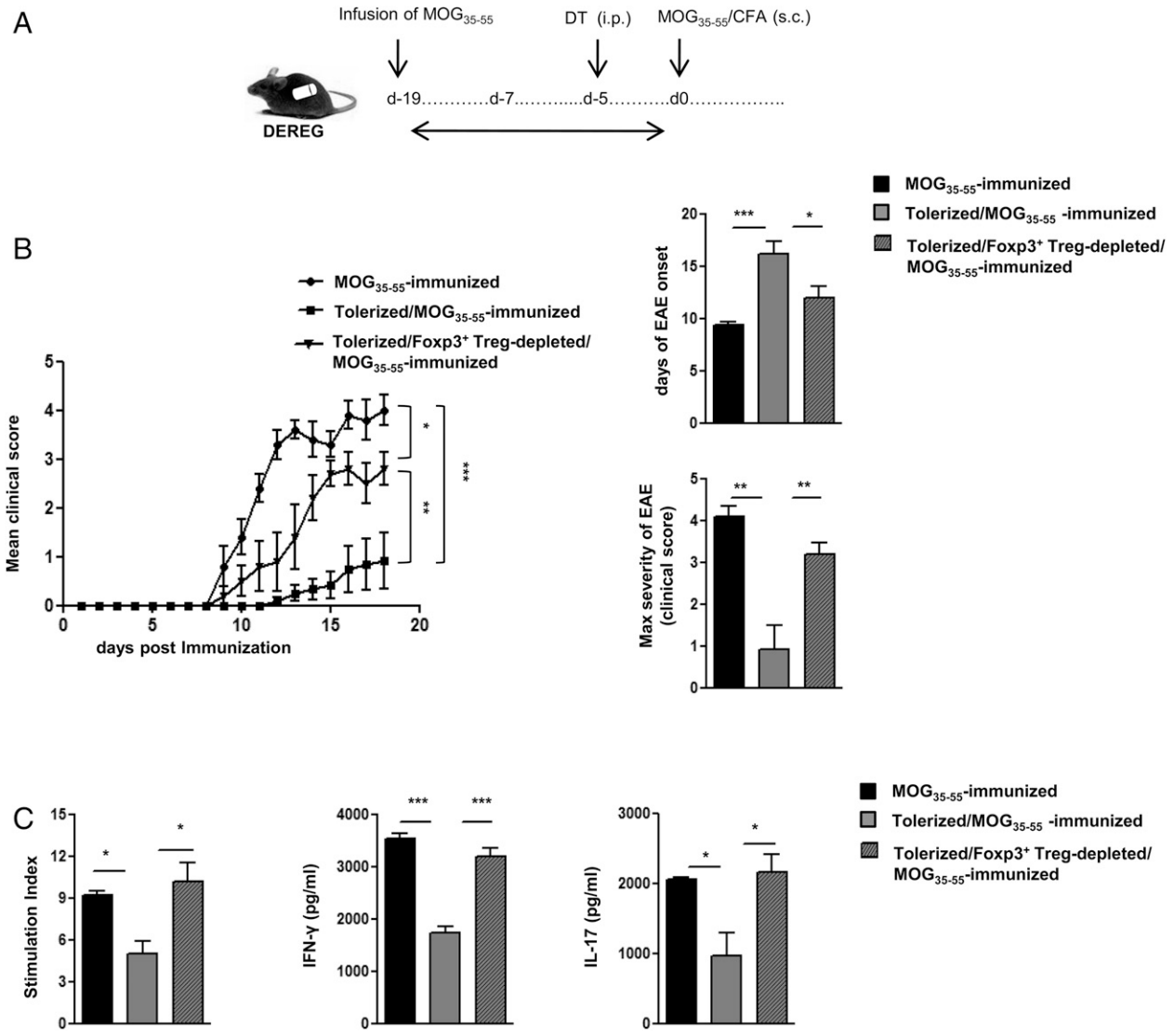

FIGURE 3. Operation of dominant tolerance executed by $MOG_{35–55}$-specific $Foxp3^+$ Tregs in tolerized mice. (**A**) Protocol for depletion of $Foxp3^+$ Tregs in $MOG_{35–55}$-infused DEREG mice. (**B**) Mean clinical score (***$p < 0.0001$, **$p = 0.0072$, *$p = 0.0269$), days of onset (***$p = 0.0004$, *$p = 0.0285$), and EAE severity (**$p = 0.0012$, **$p = 0.0087$) are shown. (**C**) Stimulation index (*$p = 0.0335$, *$p = 0.0111$) and levels of IFN-γ (***$p < 0.0001$, ***$p = 0.0005$, ***$p = 0.0004$) and IL-17 (**$p = 0.004$, **$p = 0.0085$, **$p = 0.0031$) as in Fig. 1B. Results are expressed as means ± SEM; $n = 8$ mice/group, three independent experiments.

suggesting that IL-10 inhibits CCR7 expression on iDCs. Additionally, $MOG_{35–55}$-immunized $Il10^{-/-}$ mice exhibited elevated numbers of iDCs in their dLNs compared with their WT littermates (Fig. 7D) that was accompanied by enhanced expression of CCR7 on iDCs (Fig. 7E), confirming thus that IL-10 affects the recruitment of iDCs in the dLNs though regulation of CCR7 expression.

Finally, to gain insight into the molecular signaling regulating the IL-10–mediated recruitment of iDCs, we studied the expression of signaling molecules implicated in controlling CCR7-mediated chemotaxis. Generally, chemokine receptors mediate signaling via MAPKs such as JNK and p38. These molecules are important regulators of chemotaxis and random motility in a variety of cells (27–29). Chemokine receptors may also activate PI3K and the downstream effector target protein kinase B (Akt), which plays a central role in regulation of the chemotactic response in leukocytes and other cells (30, 31). We analyzed whether deficiency of IL-10 induced the activation of JNK/p38 or PI3K/Akt axis in DCs. For this, DCs were isolated from dLNs and spleen of $MOG_{35–55}$-immunized $Il10^{-/-}$ or WT littermates. The cells were lysed and the lysates were analyzed by Western blotting using Abs specific for the phosphorylated/active forms of the proteins mentioned above. Although we were not able to detect any differences in the phosphorylation pattern of MAPKs, JNK, and p38 (Fig. 7D), DCs isolated from $Il10^{-/-}$/$MOG_{35–55}$-immunized mice had increased phosphorylation of p85, the regulatory subunit of PI3K, as well as increased phosphorylation of Akt (Fig. 7D) compared with DCs isolated from $Il10^{+/+}$/$MOG_{35–55}$-immunized littermates. These data suggest that the PI3K/Akt signaling pathway is involved in the IL-10–mediated inhibition of chemotaxis in DCs.

Discussion

Foxp3-expressing Tregs play a pivotal role in the maintenance of self-tolerance, and thus methods seeking their generation and expansion are of great importance in the field of autoimmunity, where self-tolerance is disturbed. In this study, we demonstrate the de novo induction of autoantigen-specific $Foxp3^+$ Tregs in an unmanipulated immune repertoire and the concomitant induction of self-tolerance, and we provide new insights into the molecular

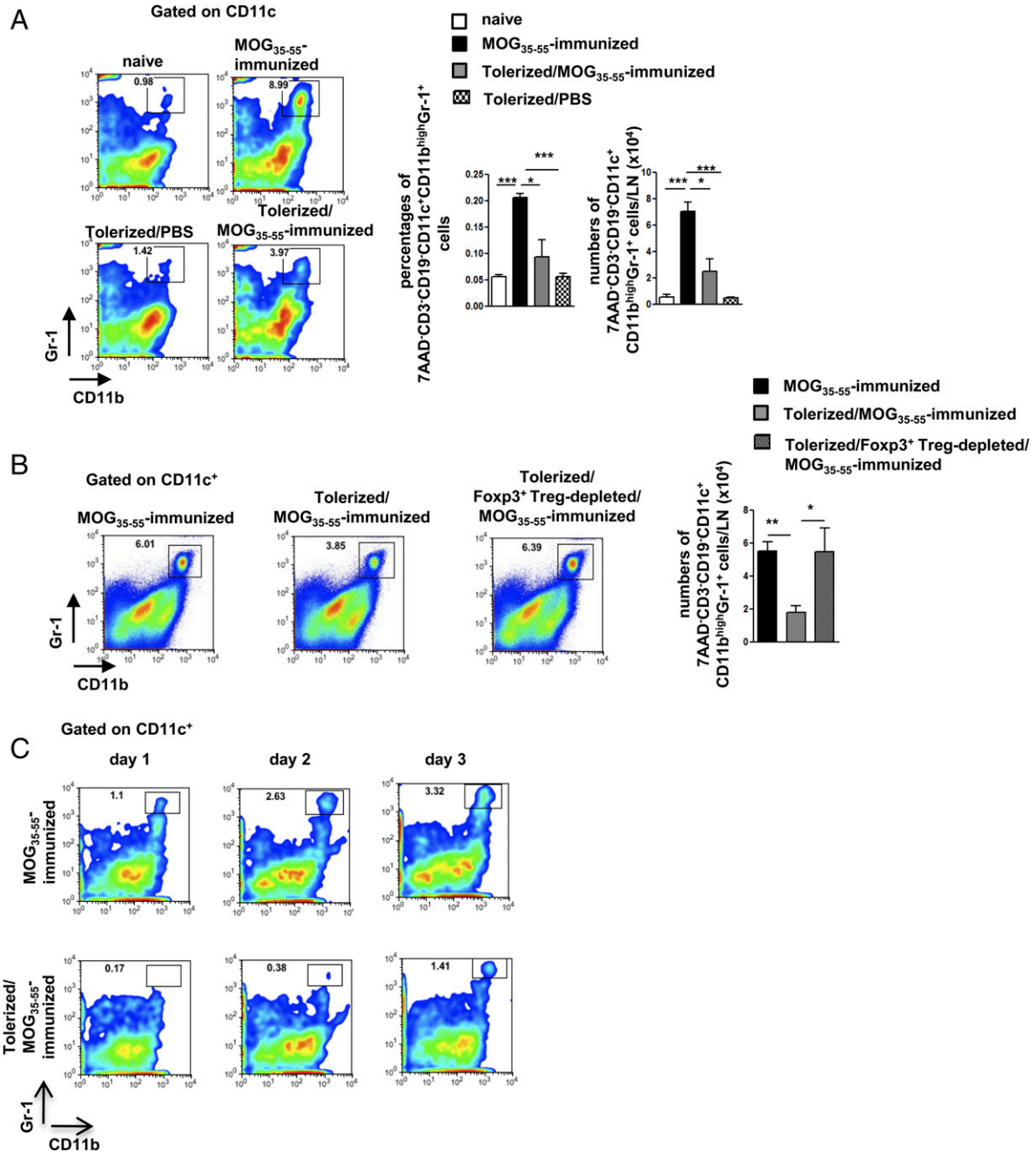

FIGURE 4. $MOG_{35–55}$-specific Foxp3$^+$ Tregs impair the accumulation of CD11c$^+$CD11b$^+$Gr-1$^+$ DCs to the dLNs. (**A**) Flow cytometric analysis of 7AAD$^-$CD3$^-$CD19$^-$CD11c$^+$CD11b^{high}Gr-1$^+$ cells in the dLNs. Percentages (*$p = 0.0260$, ***$p < 0.0001$) and numbers of 7AAD$^-$CD3$^-$CD19$^-$CD11c$^+$ CD11b^{high}Gr-1$^+$ cells (*$p = 0.0163$, ***$p = 0.0007$, ***$p = 0.0006$) per dLN are depicted. (**B**) Flow cytometric analysis and numbers (*$p = 0.0375$, **$p = 0.0028$) of CD11c$^+$CD11b^{high}Gr-1$^+$ in dLNs of $MOG_{35–55}$-immunized, tolerized/$MOG_{35–55}$-immunized, and tolerized/Foxp3$^+$ Treg-depleted/$MOG_{35–55}$-immunized DEREG mice. For (A) and (B), analysis was performed 4 d following immunization. (**C**) Kinetic analysis of 7AAD$^-$CD3$^-$CD19$^-$CD11c$^+$ CD11b^{high}Gr-1$^+$ cells in dLNs of $MOG_{35–55}$-immunized and tolerized/$MOG_{35–55}$-immunized mice 1, 2, or 3 dpi. Results are expressed as means ± SEM; $n = 6$ mice/group, three independent experiments.

and cellular bases that underlie Foxp3$^+$ Treg-mediated suppression of autoimmune responses. To this end, we demonstrate that myelin-specific Foxp3$^+$ Tregs 1) restrain the accumulation of Ag-bearing iDCs, which are required for the priming of encephalitogenic responses, in the dLNs, and 2) target the CCR7-dependent migration of iDCs in an IL-10–depedent manner.

Induction and/or expansion of Ag-specific Foxp3$^+$ Tregs has been documented in a plethora of studies. To this end, oral administration or i.v. injection of myelin peptides induce tolerance in EAE via induction of T cell clonal anergy (32, 33) or through autoreactive T cell deletion (34), respectively. Additionally, transdermal administration of myelin peptides successfully inhibited EAE in TCR transgenic animals (35, 36). Finally, expression of Ag by tissue-resident cells or delivery of Ag by either targeting the DCs or using infusion protocols resulted in generation of Ag-specific Tregs (18, 37–39). However, to our knowledge, our study for the first time demonstrates direct evidence for the operation of dominant tolerance executed by myelin-specific Foxp3$^+$ Tregs induced in unmanipulated mice and subsequent amelioration of EAE. However, whether these methods could be

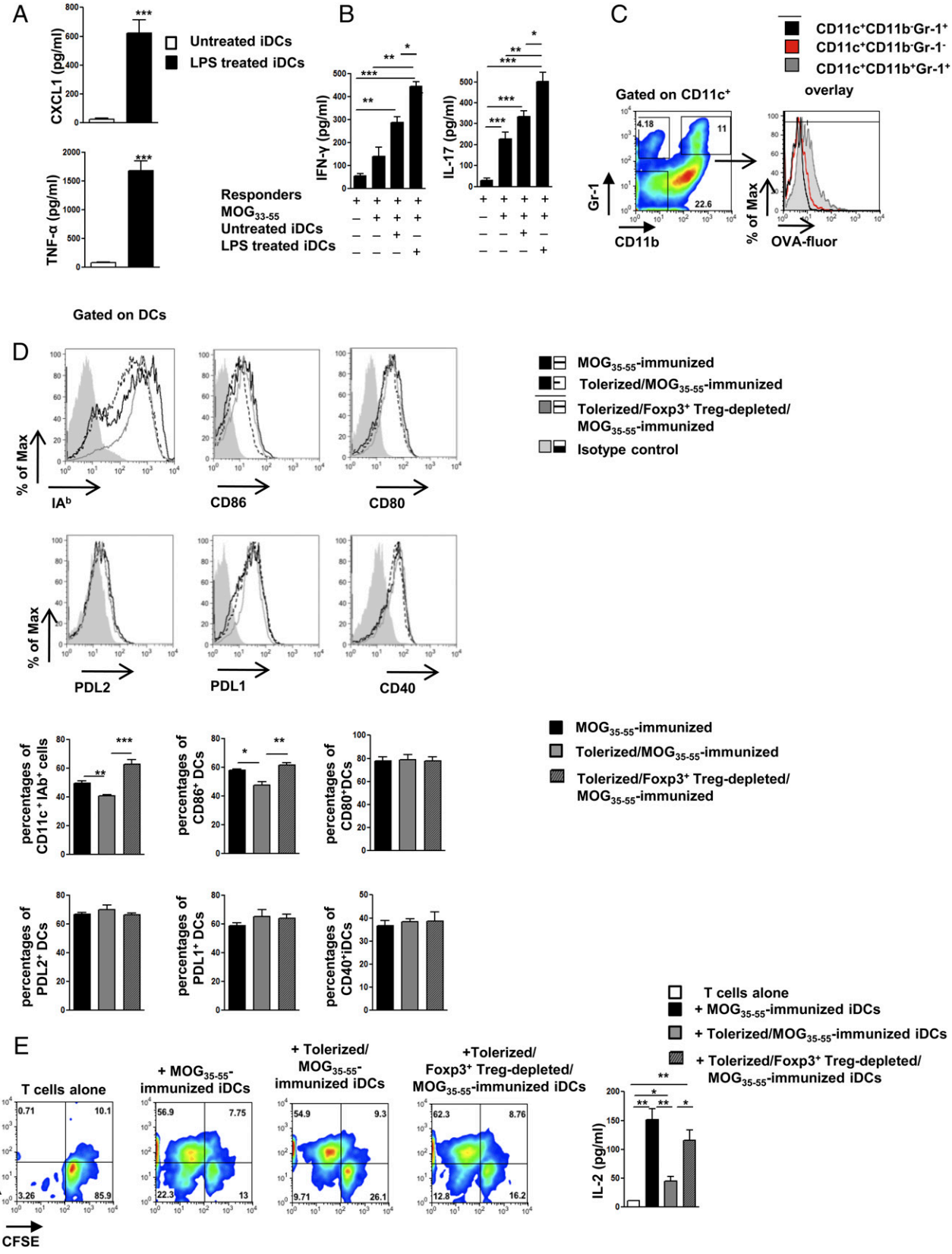

FIGURE 5. $MOG_{35–55}$-specific $Foxp3^+$ Tregs modulate the function of Ag-bearing iDCs. (**A**) Levels of CXCL1 (***$p = 0.0006$) and TNF-α (***$p = 0.0001$) in supernatants of untreated or LPS-treated purified $CD11c^+CD11b^{high}Gr\text{-}1^+$ iDCs isolated from dLNs and spleen of $MOG_{35–55}$-immunized mice. (**B**) Levels of IFN-γ (*$p = 0.0175$, **$p = 0.0017$, **$p = 0.0026$, ***$p < 0.0001$) and IL-17 (*$p = 0.0195$, **$p = 0.0016$, ***$p = 0.0006$, ***$p < 0.0001$) in supernatants from cocultures of iDCs with responder cells purified from $MOG_{35–55}$-immunized spleens and dLNs. (**C**) Flow cytometric analysis of OVA uptake in $CD11c^+$ cell subsets. (**D**) Flow cytometric analysis and percentages of $CD11c^+I\text{-}A^{bhigh}$ (**$p = 0.0016$, ***$p = 0.0005$), and expression of CD86 (*$p = 0.0203$, **$p = 0.0073$), CD40, CD80, PD-L2, and PD-L1 on $CD11c^+CD11b^+$ cells in dLNs. For data depicted in (A) and (B), results are expressed as means ± SEM; $n = 6$ mice/group, three independent experiments. (**E**) iDCs isolated from $MOG_{35–55}$-immunized, $Foxp3^+$ Treg- (*Figure legend continues*)

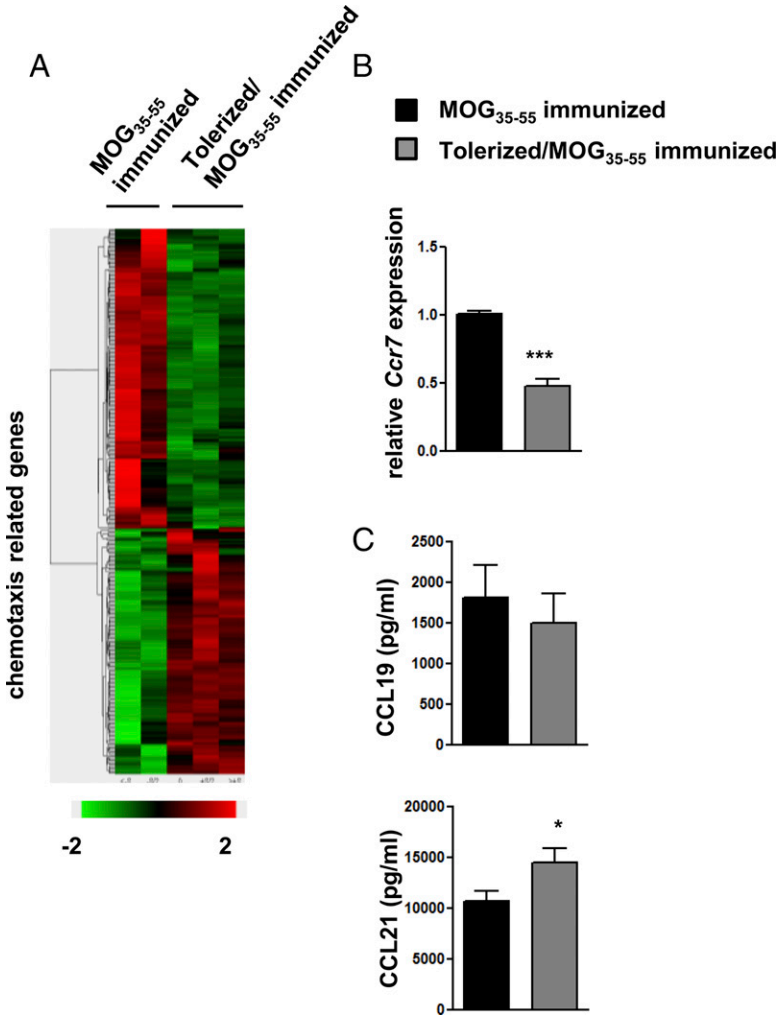

FIGURE 6. $MOG_{35–55}$-specific $Foxp3^+$ Tregs impair the accumulation of iDCs in dLNs via downregulation of CCR7 expression. (**A**) Gene expression profile of sorted iDCs (n = 2 for $MOG_{35–55}$-immunized and n = 3 for tolerized/$MOG_{35–55}$-immunized group). Hierarchical clustering of selected significant genes identified among the functional group of chemotaxis-related group was generated with Database for Annotation, Visualization and Integrated Discovery and Gene Ontology data. (**B**) Relative mRNA expression of *Ccr7* (***p = 0.0007) in iDCs. (**C**) Levels of CCL19 and CCL21 (*p = 0.0475) in supernatants of dLN homogenates. Results are expressed as means ± SEM; n = 6 mice/group, three independent experiments.

adopted to generate self-antigen–specific $Foxp3^+$ Tregs in a WT immune repertoire remains unknown. Importantly, generation of myelin-specific $Foxp3^+$ Tregs did not induce a generalized immunosuppression, because immune responses against foreign Ag were not compromised. In line with this result, Kasagi et al. (40) recently demonstrated that radiation-triggered apoptosis results in autoantigen-specific Tregs that treat ongoing autoimmunity without affecting immune responses to bacterial Ags.

Our observations raise important questions regarding the relative contribution of other Treg subsets in amelioration of EAE and establishment of self-tolerance. Notably, in our model the disease induced in tolerized mice upon elimination of myelin-specific $Foxp3^+$ Tregs appeared to be less aggressive and less severe compared with control-immunized animals, suggesting the operation of additional mechanisms of tolerance. Additionally, the increased frequency of the IL-10–producing Foxp3-GFP^- T cell population in tolerant mice suggests a possible role of peripherally induced Tr1-like suppressor cells (41, 42) in the amelioration of disease. Although, whether IL-$10^+Foxp3^-CD4^+$ T cells in tolerized mice are indeed suppressive and involved in the re-establishment of self-tolerance has not been examined; however, recent evidence demonstrated that both natural $Foxp3^+$ and induced Tregs are required for operation of tolerance (43). The mechanisms underlying the induction of IL-10–producing Tr1-like cells remain largely unknown. It is possible that myelin peptide uptake by immature or semimature APCs could instruct the induction of myelin-specific Tr1 cells in the periphery of infused mice that act in concert with thymus-derived myelin-specific $Foxp3^+$ Tregs toward the re-establishment of self-tolerance. In support of this idea, it has been demonstrated that the maturation status of DCs could direct the induction of IL-10–producing Tregs both in vivo and in vitro (44, 45). Regardless of the relative contribution of distinct cell-intrinsic mechanisms of tolerance or inducible Treg subsets in the re-establishment of self-tolerance in our model, our results clearly demonstrate that myelin-specific $Foxp3^+$ Tregs possess a central role in the re-establishment of self-tolerance by suppressing the migration of Ag-bearing iDCs in the dLNs of tolerant mice.

The Treg-mediated suppression of DC activation and function has been extensively proposed based on in vitro (46–48) and in vivo studies (49, 50). However, the DC lineage is heterogeneous and the precise subset that is targeted by Tregs is unknown. Furthermore, different DC subsets might be involved in tolerance induction in different inflammatory settings or at different inter-

depleted or not, tolerized/$MOG_{35–55}$-immunized mice ($H\text{-}2^b$) were mixed with allogeneic CFSE-labeled dLNCs ($H\text{-}2^d$) to a 1:1 ratio. CFSE dilution and CD44 expression were analyzed by flow cytometry. Levels of IL-2 were measured in culture supernatants (*p = 0.0172, *p = 0.0213, **p = 0.0017, **p = 0.0038, **p = 0.0066). Results are expressed as means ± SEM; n = 4 mice/group, three independent experiments. For (A)–(E), analysis or isolation of dLNCs was performed 3.5 dpi.

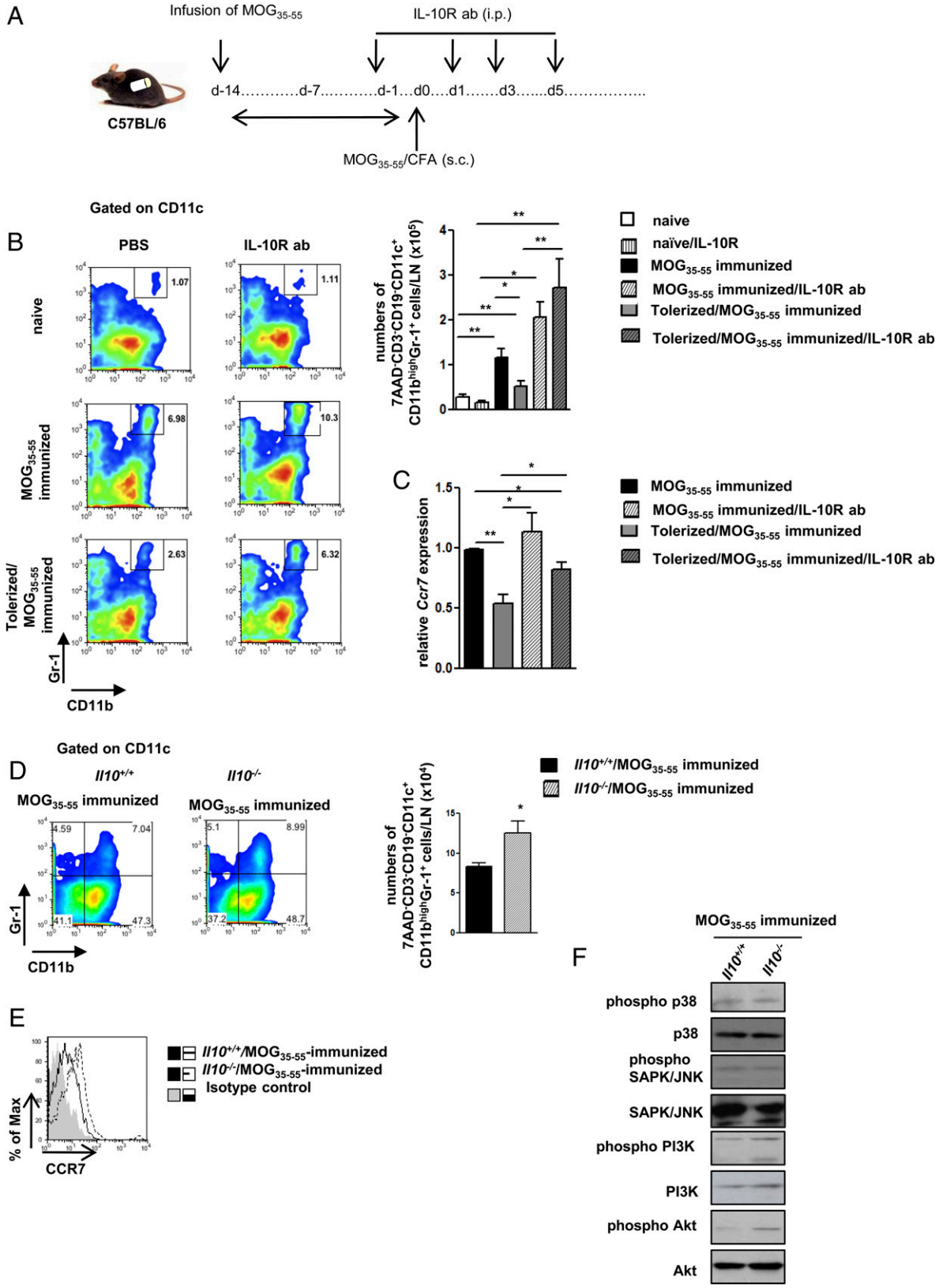

FIGURE 7. IL-10 impairs the accumulation of iDCs in the dLNs of self-tolerant mice via modulation of CCR7 signaling. (**A**) Protocol used for administration of IL-10R Ab. (**B**) Flow cytometric analysis of iDCs in the dLNs following IL-10R Ab administration. Numbers of iDCs (*p = 0.0243, *p = 0.0219, **p = 0.0099, **p = 0.0025, **p = 0.0016, **p = 0.0091) per dLN are shown. (**C**) Relative mRNA expression of *Ccr7* (*p = 0.0327, *p = 0.0145, *p = 0.0304, **p = 0.0015) in iDCs. (**D**) Flow cytometric analysis and numbers (*p = 0.0166) of iDCs in dLNs of MOG_{35-55}-immunized $Il10^{-/-}$ and $Il10^{+/+}$ mice (3 dpi). (**E**) Flow cytometric analysis of $CD11c^{+}CD11b^{high}Gr\text{-}1^{+}CCR7^{+}$ iDCs in dLNs of MOG_{35-55}-immunized $Il10^{-/-}$ and $Il10^{+/+}$ mice (3 dpi). (**F**) Western blot analysis for expression of p-p38, total p38, p-SAPK/JNK, total SAPK/JNK, p-PI3K, total pI3K, p-Akt, and total Akt in DC lysates isolated from spleens and dLNs of MOG_{35-55}-immunized $Il10^{-/-}$ and $Il10^{+/+}$ mice (3 dpi). Results are expressed as means ± SEM; n = 6 mice/group, three independent experiments.

faces. Our data reveal that self-antigen–specific Foxp3$^+$ Tregs diminish the accumulation of CD11c$^+$CD11b^{hi}Gr-1$^+$ iDCs that carry Ag to the dLNs. iDCs secrete significant amounts of proinflammatory cytokines and endow $MOG_{35–55}$-specific Th1 and Th17 responses, confirming their robust inflammatory properties (21). Furthermore, iDCs are absent from the dLNs during the steady-state and they gradually appear upon encountering the inflammatory insult. Because migration of Ag-bearing DCs to peripheral lymphoid compartments plays an essential role in the initiation of adaptive immune responses (51, 52), we propose that in our model myelin-specific Foxp3$^+$ Tregs exert their function at least by affecting the trafficking of iDCs. Additionally, iDC levels were restored in dLNs of tolerized animals upon Foxp3$^+$ Treg depletion. Finally, DNA microarrays of iDCs isolated from the dLNs of tolerized mice demonstrated a significant enrichment in genes closely linked to cell migration. Specifically, our results demonstrated that the expression of *ccr7*, required for DC mobilization to LNs (53), was significantly downregulated in iDCs from tolerant mice compared with iDCs from control animals.

How Foxp3$^+$ Tregs impair the iDC trafficking at a molecular level is not known. Our results demonstrate that in vivo neutralization of IL-10 signaling in tolerized animals is essential for restoring the iDC levels to dLNs, and this was accompanied by increased levels of CCR7 expression by iDCs. CCR7-mediated migration of DCs to dLNs is pivotal for the initiation of an immune response (23, 54). Both CCL19 and CCL21, which are known to orchestrate DC migration to LNs (55), were not reduced in LN homogenates of tolerant mice, suggesting that the impaired iDC migration to LNs could not be attributed to differences in the expression of CCR7 ligands and points toward differences in the molecular pathways downstream of CCR7. CCR7 stimulation leads to phospholipase C activation followed by diacylglycerol-mediated activation of protein kinase C and intracellular calcium release (56). Following this, a variety of signaling molecules have been implicated in the CCR7-mediated chemotaxis of DCs as well as their migratory speed. To this end, activation of PI3K and the downstream target protein Akt have been shown to coordinate chemotactic responses of inflammatory cells (30). Additionally, MAPKs have also been implicated in the regulation of chemotaxis as well as in cell motility (57). Whether IL-10 affects any of these pathways and thus DC chemotaxis remains elusive. Our results highlight that IL-10 regulates the PI3K/Akt pathway in iDCs during $MOG_{35–55}$/CFA immunization, suggesting that this pathway might be crucial for the coordinated chemotaxis and/or migratory speed of iDCs in our model. Taking into account the several DC subtypes, it is possible that different signaling events under specific inflammatory environments could operate to facilitate the DC migration and positioning into the dLNs.

In summary, our results suggest a model for the de novo generation of self-antigen–specific Foxp3$^+$ Tregs in unmanipulated mice and provide evidence for the Ag-bearing iDCs as a target of the Foxp3$^+$ Treg-mediated induction of self-tolerance. Protocols aiming at the induction and/or expansion of self-antigen–specific Foxp3$^+$ Tregs provide invaluable knowledge toward the design of cell-based therapies in autoimmune diseases that could confer specificity avoiding a pan-immunosuppression. Importantly, these findings have the potential of extending beyond the autoimmunity field to allergic responses, graft-versus-host disease, and solid organ rejections during transplantation regimens whereby disturbed tolerance is a common denominator.

Acknowledgments

We thank Eirini Kirmizi and Maria Savvaki for assisting with experiments, Xara Vlata and Niki Goulanaki for cell sorting, Anna Agapaki for histology preparations, Heidi Schliemann for chip hybridizations, and Vily Panoutsakopoulou for discussions and for critically reading the manuscript.

Disclosures

The authors have no financial conflicts of interest.

References

1. Sakaguchi, S., T. Yamaguchi, T. Nomura, and M. Ono. 2008. Regulatory T cells and immune tolerance. *Cell* 133: 775–787.
2. Littman, D. R., and A. Y. Rudensky. 2010. Th17 and regulatory T cells in mediating and restraining inflammation. *Cell* 140: 845–858.
3. Khattri, R., T. Cox, S. A. Yasayko, and F. Ramsdell. 2003. An essential role for Scurfin in CD4$^+$CD25$^+$ T regulatory cells. *Nat. Immunol.* 4: 337–342.
4. Bennett, C. L., J. Christie, F. Ramsdell, M. E. Brunkow, P. J. Ferguson, L. Whitesell, T. E. Kelly, F. T. Saulsbury, P. F. Chance, and H. D. Ochs. 2001. The immune dysregulation, polyendocrinopathy, enteropathy, X-linked syndrome (IPEX) is caused by mutations of FOXP3. *Nat. Genet.* 27: 20–21.
5. Wildin, R. S., F. Ramsdell, J. Peake, F. Faravelli, J. L. Casanova, N. Buist, E. Levy-Lahad, M. Mazzella, O. Goulet, L. Perroni, et al. 2001. X-linked neonatal diabetes mellitus, enteropathy and endocrinopathy syndrome is the human equivalent of mouse scurfy. *Nat. Genet.* 27: 18–20.
6. Korn, T., J. Reddy, W. Gao, E. Bettelli, A. Awasthi, T. R. Petersen, B. T. Bäckström, R. A. Sobel, K. W. Wucherpfennig, T. B. Strom, et al. 2007. Myelin-specific regulatory T cells accumulate in the CNS but fail to control autoimmune inflammation. *Nat. Med.* 13: 423–431.
7. Bilate, A. B., and J. J. Lafaille. 2011. It takes two to tango. *Immunity* 35: 6–8.
8. Curotto de Lafaille, M. A., and J. J. Lafaille. 2009. Natural and adaptive Foxp3$^+$ regulatory T cells: more of the same or a division of labor? *Immunity* 30: 626–635.
9. Zhou, X., S. L. Bailey-Bucktrout, L. T. Jeker, C. Penaranda, M. Martínez-Llordella, M. Ashby, M. Nakayama, W. Rosenthal, and J. A. Bluestone. 2009. Instability of the transcription factor Foxp3 leads to the generation of pathogenic memory T cells in vivo. *Nat. Immunol.* 10: 1000–1007.
10. Shevach, E. M. 2009. Mechanisms of Foxp3$^+$ T regulatory cell-mediated suppression. *Immunity* 30: 636–645.
11. von Boehmer, H. 2005. Mechanisms of suppression by suppressor T cells. *Nat. Immunol.* 6: 338–344.
12. Ioannou, M., T. Alissafi, I. Lazaridis, G. Deraos, J. Matsoukas, A. Gravanis, V. Mastorodemos, A. Plaitakis, A. Sharpe, D. Boumpas, and P. Verginis. 2012. Crucial role of granulocytic myeloid-derived suppressor cells in the regulation of central nervous system autoimmune disease. *J. Immunol.* 188: 1136–1146.
13. Menssen, A., G. Edinger, J. R. Grün, U. Haase, R. Baumgrass, A. Grützkau, A. Radbruch, G. R. Burmester, and T. Häupl. 2009. SiPaGene: a new repository for instant online retrieval, sharing and meta-analyses of GeneChip expression data. *BMC Genomics* 10: 98.
14. Bluestone, J. A., and Q. Tang. 2004. Therapeutic vaccination using CD4$^+$CD25$^+$ antigen-specific regulatory T cells. *Proc. Natl. Acad. Sci. USA* 101(Suppl. 2): 14622–14626.
15. Klein, L., K. Khazaie, and H. von Boehmer. 2003. In vivo dynamics of antigen-specific regulatory T cells not predicted from behavior in vitro. *Proc. Natl. Acad. Sci. USA* 100: 8886–8891.
16. Apostolou, I., and H. von Boehmer. 2004. In vivo instruction of suppressor commitment in naive T cells. *J. Exp. Med.* 199: 1401–1408.
17. Daniel, C., B. Weigmann, R. Bronson, and H. von Boehmer. 2011. Prevention of type 1 diabetes in mice by tolerogenic vaccination with a strong agonist insulin mimetope. *J. Exp. Med.* 208: 1501–1510.
18. Verginis, P., K. A. McLaughlin, K. W. Wucherpfennig, H. von Boehmer, and I. Apostolou. 2008. Induction of antigen-specific regulatory T cells in wild-type mice: visualization and targets of suppression. *Proc. Natl. Acad. Sci. USA* 105: 3479–3484.
19. Ioannou, M., T. Alissafi, L. Boon, D. Boumpas, and P. Verginis. 2013. In vivo ablation of plasmacytoid dendritic cells inhibits autoimmunity through expansion of myeloid-derived suppressor cells. *J. Immunol.* 190: 2631–2640.
20. León, B., M. López-Bravo, and C. Ardavín. 2007. Monocyte-derived dendritic cells formed at the infection site control the induction of protective T helper 1 responses against *Leishmania*. *Immunity* 26: 519–531.
21. Nakano, H., K. L. Lin, M. Yanagita, C. Charbonneau, D. N. Cook, T. Kakiuchi, and M. D. Gunn. 2009. Blood-derived inflammatory dendritic cells in lymph nodes stimulate acute T helper type 1 immune responses. *Nat. Immunol.* 10: 394–402.
22. Qu, C., E. W. Edwards, F. Tacke, V. Angeli, J. Llodrá, G. Sanchez-Schmitz, A. Garin, N. S. Haque, W. Peters, N. van Rooijen, et al. 2004. Role of CCR8 and other chemokine pathways in the migration of monocyte-derived dendritic cells to lymph nodes. *J. Exp. Med.* 200: 1231–1241.
23. Förster, R., A. Schubel, D. Breitfeld, E. Kremmer, I. Renner-Müller, E. Wolf, and M. Lipp. 1999. CCR7 coordinates the primary immune response by establishing functional microenvironments in secondary lymphoid organs. *Cell* 99: 23–33.

24. Li, M. O., Y. Y. Wan, S. Sanjabi, A. K. Robertson, and R. A. Flavell. 2006. Transforming growth factor-β regulation of immune responses. *Annu. Rev. Immunol.* 24: 99–146.
25. Maynard, C. L., and C. T. Weaver. 2008. Diversity in the contribution of interleukin-10 to T-cell-mediated immune regulation. *Immunol. Rev.* 226: 219–233.
26. Moore, K. W., R. de Waal Malefyt, R. L. Coffman, and A. O'Garra. 2001. Interleukin-10 and the interleukin-10 receptor. *Annu. Rev. Immunol.* 19: 683–765.
27. Wong, M. M., and E. N. Fish. 2003. Chemokines: attractive mediators of the immune response. *Semin. Immunol.* 15: 5–14.
28. Klemke, R. L., S. Cai, A. L. Giannini, P. J. Gallagher, P. de Lanerolle, and D. A. Cheresh. 1997. Regulation of cell motility by mitogen-activated protein kinase. *J. Cell Biol.* 137: 481–492.
29. Huang, C., Z. Rajfur, C. Borchers, M. D. Schaller, and K. Jacobson. 2003. JNK phosphorylates paxillin and regulates cell migration. *Nature* 424: 219–223.
30. Sotsios, Y., and S. G. Ward. 2000. Phosphoinositide 3-kinase: a key biochemical signal for cell migration in response to chemokines. *Immunol. Rev.* 177: 217–235.
31. Curnock, A. P., M. K. Logan, and S. G. Ward. 2002. Chemokine signalling: pivoting around multiple phosphoinositide 3-kinases. *Immunology* 105: 125–136.
32. Friedman, A., and H. L. Weiner. 1994. Induction of anergy or active suppression following oral tolerance is determined by antigen dosage. *Proc. Natl. Acad. Sci. USA* 91: 6688–6692.
33. Weiner, H. L., A. Friedman, A. Miller, S. J. Khoury, A. al-Sabbagh, L. Santos, M. Sayegh, R. B. Nussenblatt, D. E. Trentham, and D. A. Hafler. 1994. Oral tolerance: immunologic mechanisms and treatment of animal and human organ-specific autoimmune diseases by oral administration of autoantigens. *Annu. Rev. Immunol.* 12: 809–837.
34. Leadbetter, E. A., C. R. Bourque, B. Devaux, C. D. Olson, G. H. Sunshine, S. Hirani, B. P. Wallner, D. E. Smilek, and M. P. Happ. 1998. Experimental autoimmune encephalomyelitis induced with a combination of myelin basic protein and myelin oligodendrocyte glycoprotein is ameliorated by administration of a single myelin basic protein peptide. *J. Immunol.* 161: 504–512.
35. Bynoe, M. S., J. T. Evans, C. Viret, and C. A. Janeway, Jr. 2003. Epicutaneous immunization with autoantigenic peptides induces T suppressor cells that prevent experimental allergic encephalomyelitis. *Immunity* 19: 317–328.
36. Szczepanik, M., M. Tutaj, K. Bryniarski, and B. N. Dittel. 2005. Epicutaneously induced TGF-β-dependent tolerance inhibits experimental autoimmune encephalomyelitis. *J. Neuroimmunol.* 164: 105–114.
37. Sela, U., P. Olds, A. Park, S. J. Schlesinger, and R. M. Steinman. 2011. Dendritic cells induce antigen-specific regulatory T cells that prevent graft versus host disease and persist in mice. *J. Exp. Med.* 208: 2489–2496.
38. Jordan, M. S., A. Boesteanu, A. J. Reed, A. L. Petrone, A. E. Holenbeck, M. A. Lerman, A. Naji, and A. J. Caton. 2001. Thymic selection of CD4+CD25+ regulatory T cells induced by an agonist self-peptide. *Nat. Immunol.* 2: 301–306.
39. Kretschmer, K., I. Apostolou, D. Hawiger, K. Khazaie, M. C. Nussenzweig, and H. von Boehmer. 2005. Inducing and expanding regulatory T cell populations by foreign antigen. *Nat. Immunol.* 6: 1219–1227.
40. Kasagi, S., P. Zhang, L. Che, B. Abbatiello, T. Maruyama, H. Nakatsukasa, P. Zanvit, W. Jin, J. E. Konkel, and W. Chen. 2014. In vivo-generated antigen-specific regulatory T cells treat autoimmunity without compromising antibacterial immune response. *Sci. Transl. Med.* 6: 241ra278.
41. Battaglia, M., S. Gregori, R. Bacchetta, and M. G. Roncarolo. 2006. Tr1 cells: from discovery to their clinical application. *Semin. Immunol.* 18: 120–127.
42. Roncarolo, M. G., S. Gregori, M. Battaglia, R. Bacchetta, K. Fleischhauer, and M. K. Levings. 2006. Interleukin-10-secreting type 1 regulatory T cells in rodents and humans. *Immunol. Rev.* 212: 28–50.
43. Haribhai, D., J. B. Williams, S. Jia, D. Nickerson, E. G. Schmitt, B. Edwards, J. Ziegelbauer, M. Yassai, S. H. Li, L. M. Relland, et al. 2011. A requisite role for induced regulatory T cells in tolerance based on expanding antigen receptor diversity. *Immunity* 35: 109–122.
44. Levings, M. K., S. Gregori, E. Tresoldi, S. Cazzaniga, C. Bonini, and M. G. Roncarolo. 2005. Differentiation of Tr1 cells by immature dendritic cells requires IL-10 but not $CD25^+CD4^+$ Tr cells. *Blood* 105: 1162–1169.
45. Verginis, P., H. S. Li, and G. Carayanniotis. 2005. Tolerogenic semimature dendritic cells suppress experimental autoimmune thyroiditis by activation of thyroglobulin-specific $CD4^+CD25^+$ T cells. *J. Immunol.* 174: 7433–7439.
46. Cederbom, L., H. Hall, and F. Ivars. 2000. $CD4^+CD25^+$ regulatory T cells down-regulate co-stimulatory molecules on antigen-presenting cells. *Eur. J. Immunol.* 30: 1538–1543.
47. Veldhoen, M., H. Moncrieffe, R. J. Hocking, C. J. Atkins, and B. Stockinger. 2006. Modulation of dendritic cell function by naive and regulatory $CD4^+$ T cells. *J. Immunol.* 176: 6202–6210.
48. Misra, N., J. Bayry, S. Lacroix-Desmazes, M. D. Kazatchkine, and S. V. Kaveri. 2004. Cutting edge: human $CD4^+CD25^+$ T cells restrain the maturation and antigen-presenting function of dendritic cells. *J. Immunol.* 172: 4676–4680.
49. Tadokoro, C. E., G. Shakhar, S. Shen, Y. Ding, A. C. Lino, A. Maraver, J. J. Lafaille, and M. L. Dustin. 2006. Regulatory T cells inhibit stable contacts between $CD4^+$ T cells and dendritic cells in vivo. *J. Exp. Med.* 203: 505–511.
50. Tang, Q., J. Y. Adams, A. J. Tooley, M. Bi, B. T. Fife, P. Serra, P. Santamaria, R. M. Locksley, M. F. Krummel, and J. A. Bluestone. 2006. Visualizing regulatory T cell control of autoimmune responses in nonobese diabetic mice. *Nat. Immunol.* 7: 83–92.
51. Banchereau, J., and R. M. Steinman. 1998. Dendritic cells and the control of immunity. *Nature* 392: 245–252.
52. King, I. L., M. A. Kroenke, and B. M. Segal. 2010. GM-CSF-dependent, $CD103^+$ dermal dendritic cells play a critical role in Th effector cell differentiation after subcutaneous immunization. *J. Exp. Med.* 207: 953–961.
53. Förster, R., A. C. Davalos-Misslitz, and A. Rot. 2008. CCR7 and its ligands: balancing immunity and tolerance. *Nat. Rev. Immunol.* 8: 362–371.
54. MartIn-Fontecha, A., S. Sebastiani, U. E. Höpken, M. Uguccioni, M. Lipp, A. Lanzavecchia, and F. Sallusto. 2003. Regulation of dendritic cell migration to the draining lymph node: impact on T lymphocyte traffic and priming. *J. Exp. Med.* 198: 615–621.
55. Rot, A., and U. H. von Andrian. 2004. Chemokines in innate and adaptive host defense: basic chemokinese grammar for immune cells. *Annu. Rev. Immunol.* 22: 891–928.
56. Wu, D., C. K. Huang, and H. Jiang. 2000. Roles of phospholipid signaling in chemoattractant-induced responses. *J. Cell Sci.* 113: 2935–2940.
57. Riol-Blanco, L., N. Sánchez-Sánchez, A. Torres, A. Tejedor, S. Narumiya, A. L. Corbí, P. Sánchez-Mateos, and J. L. Rodríguez-Fernández. 2005. The chemokine receptor CCR7 activates in dendritic cells two signaling modules that independently regulate chemotaxis and migratory speed. *J. Immunol.* 174: 4070–4080.